

# Rational Design of Atomic Layers of Pt Cluster Anchored on Mo<sub>2</sub>C Nanorods for Efficient Hydrogen Evolution over a Wide pH Range

Yu Qiu,<sup>a\*</sup> Zhilin Wen,<sup>b\*</sup> Chaoran Jiang,<sup>c</sup> Xiaojun Wu,<sup>b</sup> Rui Si,<sup>d</sup> Jun Bao,<sup>e</sup> Qinghua Zhang,<sup>f</sup> Lin Gu,<sup>f</sup> Junwang Tang<sup>c\*</sup> and Xiaohui Guo<sup>a\*</sup>

Transition metal carbide (TMC) compound has been extensively investigated as a catalyst such as for hydrogenation due to its noble metal-like properties. However its activity in electrocatalytic water splitting is very moderate, which is of great importance for energy storage. Herein we applied a novel strategy to make atomic layers Pt clusters anchored on Mo<sub>2</sub>C nanorods (Pt/Mo<sub>2</sub>C) functions as a high-performance and robust catalyst for hydrogen evolution. The optimized 1.08 wt% Pt/ Mo<sub>2</sub>C exhibits 25 folds, 10 folds and 15 folds better mass activity than the widely used reference 20 wt% Pt/C in neutral, acidic (pH = 0.3), and alkaline media (pH = 14), respectively. This catalyst also represents nearly 0 V onset potential and an extremely low overpotential of -8.3 mV at current density of 10 mA cm<sup>-2</sup>, far better than the majority of reported electrocatalysts including the commercial reference catalyst (20 wt%) Pt/C. Further it represents an outstanding long-term operational durability of 120 hours. Theoretical calculation predicts that the ultrathin layer of Pt clusters on Mo-Mo<sub>2</sub>C yields the lowest absolute value of  $\Delta G_{H^+}$ . Experimental results demonstrate that the atomic layer of Pt clusters anchored on Mo<sub>2</sub>C substrate would greatly enhance electron and mass transportation efficiency and structural stability. These findings could provide the foundation for developing highly effective and scalable hydrogen evolution catalysts.

## Introduction

Electrocatalytic water splitting has been one of the most promising routes for efficient H<sub>2</sub> production which can work as a practical way to store the excess electricity generated by solar panel, wind and nuclear reactor. Although platinum group metals (PGMs), such as platinum at present are still considered to be the state-of-art electrocatalysts for hydrogen evolution reaction (HER) due to its highly catalytic activity and stability, their activity highly depends on the mass used and lack of abundance of Pt hinder its large scale commercialization.<sup>[1-4]</sup> Therefore, considerable efforts have been focused on developing alternative catalysts to replace Pt or reducing Pt amount required.

Recently, transition metal carbides (TMCs) have been considered as one of the most promising groups of the low-cost catalysts for HER due to their Pt-like electronic structure.<sup>[5-9]</sup> In addition, TMCs have been proved as a class of catalysts, which are stable in both acidic and alkaline media under HER operation.<sup>[5]</sup> However, their intrinsic activities are still far from those Pt-based catalysts. To overcome these issues, one method of discovering cost-effective and efficient catalysts is to modify TMCs by Pt group metals as co-catalysts.<sup>[8]</sup> Chen et al. shown that Pt monolayer supported on tungsten carbide film (Pt/WC or Pt/W<sub>2</sub>C) exhibited nearly identical HER activity to that of bulk Pt foil in acidic media, whereas their low surface area limited their application on practical electrolyser devices.<sup>[7, 8]</sup> Recently, low-loading of Pt over six transition metal carbide (Pt/TMC) power catalysts including Pt/NbC, Pt/TaC, Pt/VC, Pt/ZrC, Pt/TiC and Pt/WC were synthesised and evaluated for HER performance in alkaline electrolytes. The majority of Pt/TMC catalysts in their study required a minimum loading of 5 wt% Pt to achieve comparable activity with 46 wt% Pt/C, apart from Pt on VC substrate (1 wt% Pt/VC) in 0.1 M KOH medium. However, the stability in alkaline and the performance in acidic electrolyte were

not reported. <sup>[10]</sup> Based on the density function theory (DFT) calculations of molybdenum carbides, the hybridization between d-orbital of metal molybdenum and s- and p-orbital of carbon brings about the broadening of the d-band structure of molybdenum carbides, thus leading to a similar d-band structure to Pt.<sup>[11, 12]</sup> Experimentally, Pt/Mo<sub>2</sub>C has previously been employed as a stable and efficient catalyst for cellulose conversion to polyols, water-gas shift reaction, and methanol steam reforming.<sup>[13-15]</sup> These previous work demonstrate the strong interaction and excellent synergistic effect between Pt and Mo<sub>2</sub>C supports.<sup>[7, 16]</sup> Historically, Pt/Mo<sub>2</sub>C catalysts were also investigated for HER. For instance, Li et al. reported an ALD deposited 4.4 wt% Pt nanoparticles on Mo<sub>2</sub>C supports shown a similar activity to 20 wt% Pt/C with sufficient durability in 0.5M H<sub>2</sub>SO<sub>4</sub> for 48 h.<sup>[17]</sup> Moreover, Chen et al.<sup>[18]</sup> synthesized Pt/Mo<sub>2</sub>C core-shell particles using co-impregnation method, which significant decreased the Pt loading amount to 2 wt% on Mo<sub>2</sub>C in order to achieve comparable HER activity to 10 wt% Pt/C in 0.5 M H<sub>2</sub>SO<sub>4</sub>. Inspired by such studies, synthesizing stable and atomic layers of Pt on Mo<sub>2</sub>C is very likely to be an effective method to further minimizing the Pt loading while achieving a better activity.

Among all molybdenum carbides ( $\alpha$ -Mo<sub>2</sub>C,  $\beta$ -Mo<sub>2</sub>C,  $\gamma$ -Mo<sub>2</sub>C,  $\eta$ -Mo<sub>2</sub>C),  $\beta$ -Mo<sub>2</sub>C exhibits the highest HER activity.<sup>[19]</sup> Therefore,  $\beta$ -Mo<sub>2</sub>C was employed as the support for Pt loading in this study and the nanorods of  $\beta$ -Mo<sub>2</sub>C was first prepared to maximize the reaction surface area. DFT calculation then predicted the favorable active sites for Pt/Mo<sub>2</sub>C fabrication. The desired Pt/Mo<sub>2</sub>C composites, which consist of well-dispersed atomic layers of Pt species grown on  $\beta$ -Mo<sub>2</sub>C nanorods, were then synthesized successfully. The loading amount of Pt anchored on Mo<sub>2</sub>C was minimized to 1 wt% which still shows more than one order of magnitude higher activity and extremely better stability for HER than the commercial benchmark catalyst 20 wt% Pt/C. in acidic, neutral and basic medium. The mechanism of Pt/Mo<sub>2</sub>C catalyst for excellent HER performance was also fully investigated.

## Experimental Section

**Synthesis of Mo<sub>2</sub>C support:** The Molybdenum Carbide (Mo<sub>2</sub>C) supports were synthesized via a simple thermal reduction process. In detail, 100 mg of Mo<sub>3</sub>O<sub>10</sub>(C<sub>6</sub>H<sub>8</sub>N)<sub>2</sub>·2H<sub>2</sub>O was heated in a tube furnace at 650 °C for 2 h at a rate of 2 °C · min<sup>-1</sup> under a H<sub>2</sub>/Ar flow (10% H<sub>2</sub> by volume) and naturally cooled down to room temperature afterwards.

**Synthesis of Pt/Mo<sub>2</sub>C composites:** Typically, desirable amounts of potassium platinumochloride (K<sub>2</sub>PtCl<sub>4</sub>) was first dissolved in 2 mL of ethylene glycol (EG) in a glass vial to form a homogenous solution (denoted as solution A). Secondly, the required amount of polyvinylpyrrolidone (PVP) (*M<sub>n</sub>* = 10000) was dissolved in 2 mL of EG solvent to obtain a high ratio of PVP to Pt (eg. For 1.08 wt% Pt/Mo<sub>2</sub>C sample, the ratio is 10) (denoted as solution B). Thirdly, 50 mg of Mo<sub>2</sub>C solution was dispersed in 15 mL of EG followed by ultrasonication for 10 min (denoted as solution C). Solution C was stirred vigorously for 1 h under a 100 °C oil bath. Then, solution A and solution B were simultaneously added to the solution C while very slowly to ensure Pt precursor was highly surrendered by PVP in order to obtain high dispersed and atomic level of Pt on the substrate. After stirred at 100 °C for 22 h, the precipitates were centrifuged and washed several times with absolute ethanol and dried for 12 h at 70 °C. Finally, the prepared Pt/Mo<sub>2</sub>C samples can be obtained by calcination treatment at 400 °C furnace for 3 h in Ar atmosphere. Pt/Mo<sub>2</sub>C composites with different Pt loading amounts could be synthesized via addition of different amounts of K<sub>2</sub>PtCl<sub>4</sub> precursors, noted as 1.08 wt% Pt/Mo<sub>2</sub>C, 1.78 wt% Pt/Mo<sub>2</sub>C, and 9.19 wt% Pt/Mo<sub>2</sub>C, respectively. The precise content of Pt in Pt/Mo<sub>2</sub>C was measured by ICP measurement.

**Sample characterizations:** The samples were characterized by powder X-ray diffraction (XRD) pattern using Bruker AXS-D8 diffractometer (Cu K $\alpha$  radiation,  $\lambda$  = 0.15418 nm). The chemical compositions, morphologies and the micro structures of the sample were characterized by field emission scanning electron microscopy (FESEM, Hitachi SU-8010) with an operating voltage of 5 kV, Transmission electron microscopy (TEM) equipped with energy-dispersion X-ray spectrometer (EDS) (FEI TALOS F200X at 200 kV), and X-ray photoelectron spectroscopy (BL 11U station, National synchrotron radiation lab, university of science and technology of china) was to confirm the surface electron state of the samples. Subångström resolution HAADF STEM images were obtained on a JEOL ARM200CF STEM/TEM, also equipped with a CEOS probe corrector, with a spatial resolution of 0.078 nm. Before microscopy examination, the samples were dry dispersed onto a copper grid coated with a thin holey carbon film.

**Electrochemical measurements:** All electrochemical measurements were performed using a potentiostat (VersaStudio) in a standard three electrode system using a glass carbon electrode, an Ag/AgCl electrode and a platinum foil electrode (SPI Supplies, West Chester, PA) as the working electrode, reference electrode and counter electrode, respectively. All potentials in this study were referenced to a reversible hydrogen electrode (RHE) according to  $E(\text{RHE}) = E(\text{Ag/AgCl}) + 0.21 + 0.059 \text{ pH}$ . Typically, 5 mg of catalyst and 100  $\mu\text{L}$  of 5 wt % Nafion solution were dispersed in 900  $\mu\text{L}$  of ethanol and sonicated for 30 mins to form a homogenous ink. 5  $\mu\text{L}$  of the ink was dropped cast onto a glassy carbon electrode with a diameter of 3 mm and dried at room temperature. The mass loading was 0.21 mg cm<sup>-2</sup>. Cyclic voltammetry (CV) were scanned from 0 to -0.7 V (vs Ag/AgCl) for 20 times to stabilize the current prior to the linear sweep voltammetry (LSV), which scanned from 0 to -0.7 V (vs Ag/AgCl) at room temperature in various electrolyte with different pH value (0.5 M H<sub>2</sub>SO<sub>4</sub>, pH = 0.3; 1M KOH, pH=14; or 1M potassium phosphate buffer, pH=7) at a scan rate of 5 mV s<sup>-1</sup>. The onset potential and overpotential was determined as the potential required to reach a specific current density of 1 mA cm<sup>-2</sup> and 10 mA cm<sup>-2</sup>, respectively. Electrochemical impedance spectroscopy (EIS) was performed at -0.25V overpotential with frequency from 100 KHz to 100 mHz. The stability of catalysts was tested by chronoamperometry and continuous CV (from 0 to -0.7V) cycles.

## Results & Discussion

The Gibbs free energy of H\* ( $\Delta G_{\text{H}}^*$ ) has been regarded as one of the most widely used descriptors to assess the activity of a catalyst for HER.<sup>[20]</sup> Theoretically, a promising candidate for HER is  $\Delta G_{\text{H}}^*$  value close to 0 eV, which can facilitate fast electron transfer and hydrogen release processes.<sup>[20, 21]</sup> The  $\Delta G_{\text{H}}^*$  value of the Pt/Mo<sub>2</sub>C catalysts were modeled using density functional theory

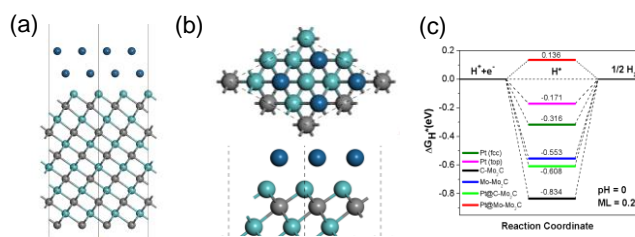
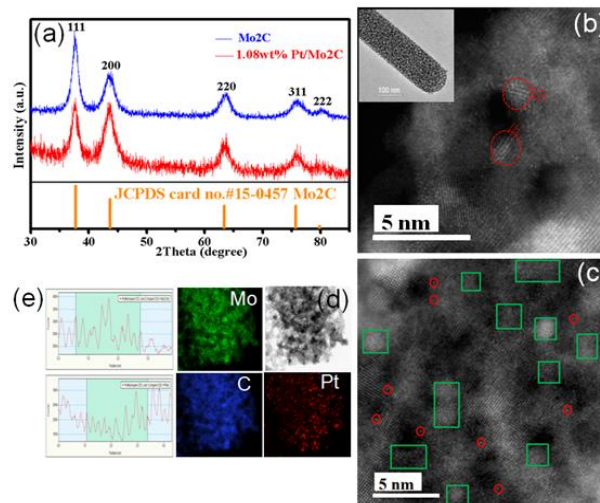


**Figure 1.** (a) Structural growth model for Mo<sub>2</sub>C and Pt. (b) Top and side view of Pt@Mo-Mo<sub>2</sub>C; Dark blue: Pt atoms, Grey: C atoms, Cyan: Mo atoms. (c) Gibbs free energy for H\* adsorption on different catalysts.

(DFT) as shown in Figure 1 a-c (see computational details in supporting information). Two possible active sites of the Pt/Mo<sub>2</sub>C have been considered, namely Pt@Mo-Mo<sub>2</sub>C and Pt@C-Mo<sub>2</sub>C. For comparison, the  $\Delta G_{H^*}$  values of Mo<sub>2</sub>C and Pt were also involved. The calculated  $\Delta G_{H^*}$  values of the most favorable active sites for Pt/Mo<sub>2</sub>C (Pt@Mo-Mo<sub>2</sub>C), Pt and Mo<sub>2</sub>C (Mo-Mo<sub>2</sub>C) are 0.136, -0.316 and -0.553 eV, respectively. Obviously, the Pt@Mo-Mo<sub>2</sub>C possess the lowest absolute value of  $\Delta G_{H^*}$ , indicating that Pt clusters on Mo<sub>2</sub>C is more beneficial to the HER process. Previous studies have shown that charge transfer at the interface plays a significant role in substrate-regulated HER enhancement.<sup>[22, 23]</sup> Hence, the charge transfer between ultrathin Pt layer and Mo-Mo<sub>2</sub>C substrate was calculated to understand the reduction of hydrogen adsorption on Pt@Mo-Mo<sub>2</sub>C. As shown in Figure S1, per Pt atom obtain 0.19 electrons from Mo<sub>2</sub>C substrate, resulting a more negative charge on adsorbed hydrogen (H\*) at Pt@Mo-Mo<sub>2</sub>C surface compared to Pt surface (0.17 electrons). Thus, the chemical adsorption of hydrogen would like to decrease because of the repulsive interaction induced by electrons injected from the substrate. To investigate the structural stability of Pt/Mo<sub>2</sub>C catalysts, we also calculated the formation energy of ultra-thin layer Pt deposited on Mo<sub>2</sub>C surface. The formation energies of ultrathin layer Pt deposited on C-terminal (C-) and Mo-terminal (Mo-) Mo<sub>2</sub>C are -0.543 and -1.051 eV per Pt atom, respectively, indicating the excellent structural stability of ultra-thin Pt cluster on Mo<sub>2</sub>C substrate, as well as the potential high loading capacity of Pt and long-term stability of HER catalytic performance.

Inspired by theoretical predictions, we have successfully synthesized ultrathin layer Pt with different loading amount on Mo<sub>2</sub>C supports using a reproducible and robust solution-based method. For comparison, the commercially available benchmark catalyst 20 wt% Pt/C was also tested for HER performance. To confirm the structure morphology and surface composition of Pt/Mo<sub>2</sub>C catalysts, a systematic process of material characterization was undertaken. The as-synthesized Pt/Mo<sub>2</sub>C catalysts were characterized by powder X-ray diffraction (XRD) firstly. The XRD results show diffraction patterns of 1.08 wt% Pt/Mo<sub>2</sub>C accurately corresponding to the hexagonal closed-packed  $\beta$ -Mo<sub>2</sub>C phase (JCPDS no. 15-0457) (Figure 2a). Noticeably, no diffraction peaks corresponding to metallic Pt, PtOx, or Pt-Mo alloy are observed, may because the amount of Pt species be below the detection limit. Transmission electron microscopy (TEM) and scanning electron microscopy (SEM) investigations were conducted to determine the structure and morphology of Pt/Mo<sub>2</sub>C. The Pt/Mo<sub>2</sub>C preserves the nanorods morphology with diameter of ca.100 nm, as indicated by TEM and SEM observation (Figure S2-S5). In Figure 2b insert, no visible Pt particles are observed in the TEM image of 1.08 wt% Pt/Mo<sub>2</sub>C, whereas the cross sectional HADDF STEM image in Figure

2b shows the ultrathin Pt layer on Mo<sub>2</sub>C surface (ca.3-4 atomic layer

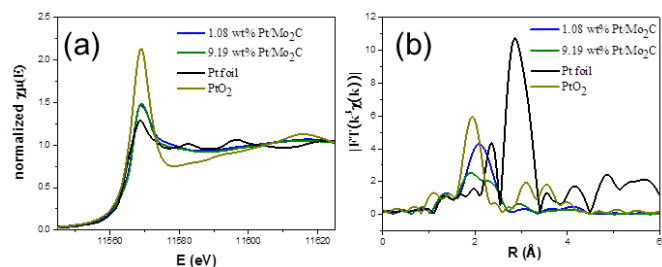


thickness). To further confirm the presence of few atomic layers Pt on the surface of the Mo<sub>2</sub>C substrate, subångström-resolution and aberration-corrected scanning transmission electron microscopy (STEM) was used to characterize the dispersion and configuration of the Pt species within the catalyst.<sup>[24, 25]</sup> Individual heavy atoms in practical catalysts can be identified via atomic-resolution high-angle annular dark-field (HAADF) imaging.<sup>[26, 27]</sup> Abundant Pt clusters (green rectangle) with size range from 0.5 - 3 nm are clearly observed in a highly dispersed form on the surface of the Mo<sub>2</sub>C support (Figure 2c).

**Figure 2.** Structure and morphology and composition characterization of 1.08 wt% Pt/Mo<sub>2</sub>C catalyst, (a) XRD patterns; (b) Cross-sectional HADDF STEM image (atomic layers of Pt species are indicated inside the red circle), the insert shows a typical TEM image; (c) HADDF STEM images (red circles indicate the single atomic Pt and green rectangles indicate the Pt clusters); (d) the EDS elemental mapping and (e) the corresponding line profiles mapping.

Moreover, some visible single atomic Pt species can be observed (red circle) in Figure 2c, indicating the coexistence of Pt clusters and single atomic Pt in the sample. The HAADF and the corresponding EDS element mapping of 1.08 wt% Pt/Mo<sub>2</sub>C reveal the homogeneous distribution of Pt, Mo and C atoms (Figure 2d and e). Even increasing the Pt loading amount to 1.78wt% and then 9.19 wt%, both samples still show much more highly dispersed Pt clusters layers and some single atomic Pt on the surface of Mo<sub>2</sub>C substrate (Figure S4 and S5d). The high densities of these highly dispersed Pt clusters anchored on Mo<sub>2</sub>C with atomic layer thickness make Pt/Mo<sub>2</sub>C a promising electrocatalyst for the HER.<sup>[28]</sup>

X-ray photoelectron spectroscopy (XPS) studies were performed to probe the surface composition and valence states of Pt/Mo<sub>2</sub>C. Figure 5c reveals that the peaks center at 71.78 eV and 72.78 eV. The latter is contributed to Pt<sup>2+</sup> states and the former is ca. 0.2 eV higher energy than metallic Pt, thus denoting Pt<sup>δ+</sup>.<sup>[29, 30]</sup> The concentration of Pt<sup>δ+</sup> and Pt<sup>2+</sup> were calculated based on the peak area. The calculated Pt<sup>δ+</sup>/Pt<sup>2+</sup> ratio is about half. Mo 3d spectrum demonstrates the contribution from Mo<sub>2</sub>C (at approximately 228.06, 228.62, and 231.35 eV) and MoO<sub>3</sub> (at approximately 235.31 and 232.23 eV) (Figure S6). Similar case can



be found for 9.19 wt% Pt/Mo<sub>2</sub>C sample (Figure S7). To further verify that 1.08 wt% Pt/Mo<sub>2</sub>C contains mainly ultrathin layer of Pt clusters throughout the whole catalyst, X-ray absorption fine structure (XAFS) spectra were measured on freshly prepared catalysts. As shown in Figure 3a, the visible green line intensities in the X-ray absorption near edge spectroscopy (XANES) profiles reflect the oxidation state of Pt in different samples<sup>[25, 31]</sup>, the spectra of two Pt/Mo<sub>2</sub>C samples are

**Figure 3.** X-ray absorption fine structure (XAFS) results: (a) Pt L3 edge XANES profiles and (b) EXAFS spectra in R space for Pt/Mo<sub>2</sub>C with different Pt loading, Pt foil and PtO<sub>2</sub> are used as references.

located between that of Pt foil and PtO<sub>2</sub> standards. Wherein, 1.08 wt% Pt/Mo<sub>2</sub>C exhibits an average oxidation state of +0.8 by the linear combination fit, indicating Pt clusters are close to metallic states. In addition, it is found from the Fourier transforms (R space, Figure 3b) of the extended X-ray absorption fine structure (EXAFS) data that, there is one prominent peak around 2.0 Å from the Pt-O contribution and a relatively weak peak around 3.0 Å for Pt-Pt shell originated from the Pt-O-Pt structure in oxidized PtOx clusters. Specifically, the Pt-O distances for 1.08 wt% Pt/Mo<sub>2</sub>C and 9.19 wt% Pt/Mo<sub>2</sub>C are 2.03 and 2.01 Å, respectively; while their coordination number is around 1.0 (Table S1). These PtOx clusters are believed due to the Pt bonding with the intermediate layer of MoO<sub>3</sub> lying on the surface of Mo<sub>2</sub>C substrate. Formation of a thin layer of MoO<sub>3</sub> was widely reported on Mo<sub>2</sub>C substrate when exposing it to air.<sup>[32]</sup> A Pt-Cl coordination was also found in Figure 3b, it is actually low valence state Pt<sup>δ+</sup> species that coordinate with Cl to form Pt-Cl (where Cl is from H<sub>2</sub>PtCl<sub>6</sub>·6H<sub>2</sub>O precursor). This is well agreed with XPS results (Figure 5c). Based on this analysis, it can be concluded that Pt clusters exist at both single atomic Pt (Pt-Cl) and very low oxidation state Pt (PtOx) species in these samples, in agreement with the HADDF-STEM results presented in Figure 2c and Figure S5d.

The HER activity of the Pt/Mo<sub>2</sub>C catalyst was assessed and compared with a most widely used and commercially available reference catalyst 20 wt% Pt/C catalyst and the pure Mo<sub>2</sub>C support. These trials were performed based on linear sweep voltammetry (LSV) measurements in aqueous 0.5 M H<sub>2</sub>SO<sub>4</sub> electrolyte at room temperature. All the potentials were referenced to a reverse hydrogen electrodes (RHE). As shown in Figure 4a, 1.08 wt%

Pt/Mo<sub>2</sub>C displays superior HER activity with nearly 0 V E<sub>onset</sub> (onset potential) and a small η<sub>10</sub> (overpotential to drive a current density of -10 mA cm<sup>-2</sup>) of -8.3 mV, surprisingly better than the commercially benchmark catalyst 20 wt% Pt/C, much lower than those pure Mo<sub>2</sub>C catalysts (E<sub>onset</sub> = 150 mV, η<sub>10</sub> = 170 mV). This large enhancement may be due to the synergic effect of highly dispersed ultrathin layer of Pt clusters and Mo<sub>2</sub>C. Figure 4b presents the Tafel slope for 1.08 wt% Pt/Mo<sub>2</sub>C, for which the value of 29.12 mV dec<sup>-1</sup> is also better than that of 20 wt% Pt/C (30.52 mV dec<sup>-1</sup>),

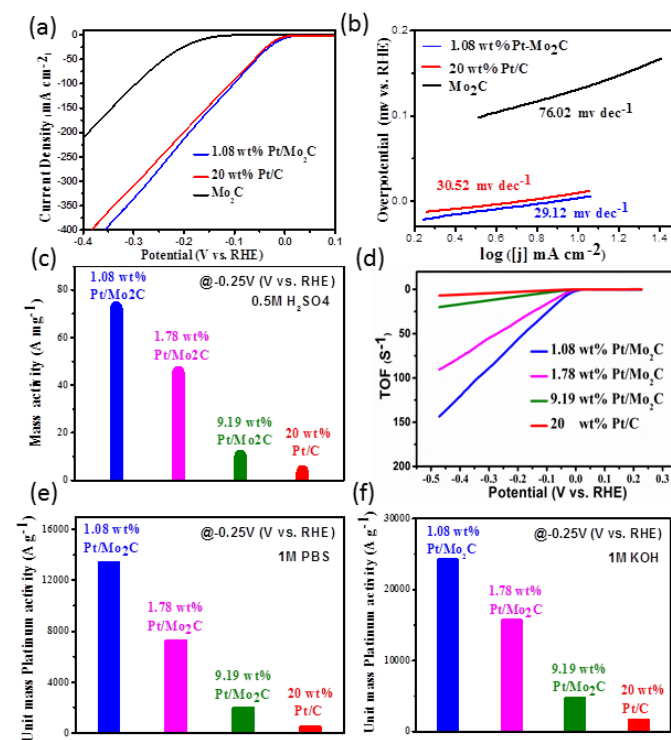


**Figure 4.** Electrocatalytic HER performance of Pt/Mo<sub>2</sub>C catalysts. Acidic media (0.5 M H<sub>2</sub>SO<sub>4</sub>): (a) HER polarization curves and (b) Tafel plots for 1.08wt % Pt/Mo<sub>2</sub>C in comparison with Mo<sub>2</sub>C and 20wt% Pt/C. (c) Mass activities and (d) TOF values for Pt/Mo<sub>2</sub>C catalysts with different Pt loading and 20 wt% Pt/C. Neutral media: (e) Mass activities of Pt/Mo<sub>2</sub>C catalysts. Alkaline media (1M KOH): (f) Mass activities of Pt/Mo<sub>2</sub>C catalysts.

and much smaller than Mo<sub>2</sub>C (76.02 mV dec<sup>-1</sup>), indicating the faster reaction kinetics due to the efficient electron transport through Mo<sub>2</sub>C to surface Pt clusters. The fast charge transfer capacity during HER also reflects on the Nyquist plots (Figure S8), for which the charge transfer resistance of the Pt/Mo<sub>2</sub>C is lower in comparison with Mo<sub>2</sub>C or 20 wt% Pt/C. Figure 4c summarizes the calculated mass activities at overpotential of -0.25 V in 0.5 M H<sub>2</sub>SO<sub>4</sub> medium, normalized to the Pt loading. The 1.08 wt.% Pt/Mo<sub>2</sub>C exhibits the highest mass activity of 75 A mg<sup>-1</sup> based on the Pt loading amount, which is nearly 10 folds greater than that obtained from 20 wt% Pt/C catalysts (7 A mg<sup>-1</sup>). These findings imply that ultrathin layer Pt cluster significantly increases the Pt utilization efficiency, and thus reduces the cost of the catalyst. To quantify the electrocatalytic activity of Pt/Mo<sub>2</sub>C, the turnover frequency (TOF) at different

overpotentials were also calculated (Figure 4d). We assume all the catalysts on the GC electrode are catalytically active for the HER. At an overpotential of  $-250$  mV, the TOF value of 1.08 wt% Pt/Mo<sub>2</sub>C ( $146$  s<sup>-1</sup>) exhibits nearly 16 folds higher than that of commercial 20 wt% Pt/C ( $9$  s<sup>-1</sup>). To further confirm the H<sub>2</sub> evolution and Faraday efficiency of Pt/Mo<sub>2</sub>C electrode, the experimental and theoretical H<sub>2</sub> evolution amount by 1.08 wt% Pt/Mo<sub>2</sub>C at a constant potential of  $-0.25$  V were performed as shown in Figure S9. The experimental H<sub>2</sub> evolution determined by gas chromatography exhibits nearly 100% Faraday efficiency when electrolysis for 110 min. Moreover, the HER performance of 1.08 wt% Pt/Mo<sub>2</sub>C was also tested in both neutral (1M PBS) and alkaline (1M KOH) condition (Figure 4 e-f and Figure S10) although in the latter case Pt is not the best one. The 1.08 wt% Pt/Mo<sub>2</sub>C shows 25 times better mass activity than the commercial 20 wt% Pt/C in neutral condition and 15 times better in the alkaline condition, respectively.

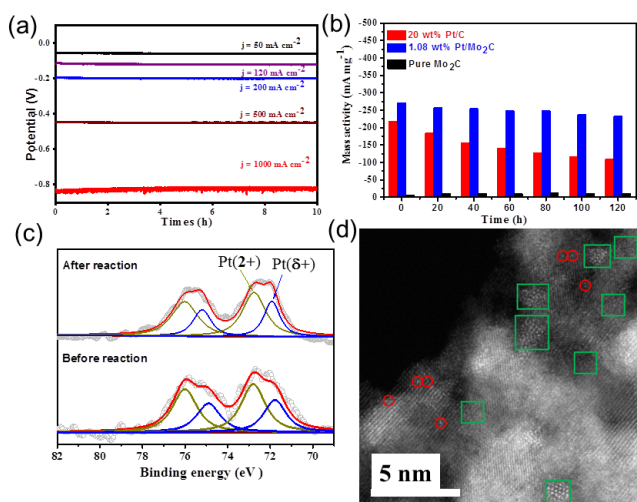


**Figure 5.** (a) Time dependence of mass activity of 1.08 wt% Pt/Mo<sub>2</sub>C, (b) V-t curves for 1.08 wt% Pt/Mo<sub>2</sub>C in comparison with pure Mo<sub>2</sub>C and 20 wt% Pt/C at different current density in 0.5 M H<sub>2</sub>SO<sub>4</sub>. (c) Comparison of Pt 4f XPS spectra for 1.08 wt% Pt/Mo<sub>2</sub>C before and after electrochemical reaction. (d) STEM bright field images of 1.08 wt% Pt/Mo<sub>2</sub>C after electrochemical reaction. Pt clusters are indicated with green rectangle, single atomic Pt is indicated with red circles.

The stability is another critical factor to evaluate the HER electrocatalyst performance. Herein, the measurement of long-term cycling stability of 1.08 wt% Pt/Mo<sub>2</sub>C shows negligible loss of the cathode current after 10000 cycles ranged from  $-0.5$ -  $0.1$ V in 0.5 M H<sub>2</sub>SO<sub>4</sub> (Figure S11), consisting with the results obtained from the chronopotentiometry curves measured at constant current density (Figure 5a). Remarkably, 1.08 wt% Pt/Mo<sub>2</sub>C catalyst exhibits no measurable loss of activity after a continuous electrolysis at constant current density ranging from 50 to 1000 mA cm<sup>-2</sup> for 10 h in 0.5 M H<sub>2</sub>SO<sub>4</sub>. The excellent durability at 1000 mA cm<sup>-2</sup> is highly beneficial to their practical applications. A further long-time test is crucial for such electrocatalyst application. We then extended the test time to 120 hours. The commercial 20 wt% Pt/C loses more than half of its initial activity,<sup>[33]</sup> while the prepared 1.08 wt% Pt/Mo<sub>2</sub>C only decays by 15% of its initial activity (Figure 5b), which are likely to be the formation of more single atomic Pt-Cl species after long-term cycles compared with before catalytic reaction, as shown in Figure 5c. Moreover, 9.19 wt% Pt/Mo<sub>2</sub>C composite

electrocatalyst also exhibits excellent stability in acidic and neutral and alkaline conditions (Figure S12). All these results have proven that Pt/Mo<sub>2</sub>C is indeed a highly efficient and stable HER electrocatalysts over a wide pH range. As to reproduce all reported record catalysts are very challenging, so far we compared our catalysts with the well-established reference 20 wt% Pt/C. To further illustrate the advance of our new catalysts, performance and experimental conditions of all reported TMCs<sup>[34-43]</sup> and/or platinum-based electrocatalysts are listed in Table S2. One can see our 1.08 wt% Pt/Mo<sub>2</sub>C catalyst is the best with respect to overpotential when the current is 10 mA/cm<sup>2</sup> (it is about  $-8.3$  mV and the second best is  $-19.7$  mV for reported PtRu@RFCs catalyst),<sup>[30]</sup> while the Tafel slope is one of the best. The structural stability of the Pt/Mo<sub>2</sub>C catalyst was further confirmed by XPS and HAADF-STEM. As shown in Figure 5c, some change could be observed from the XPS spectra of the prepared Pt/Mo<sub>2</sub>C catalyst before and after long-term cycles, namely, the calculated Pt<sup>δ+</sup>/Pt<sup>2+</sup> ratio for the post reaction sample is about 0.62, suggesting a little more single atomic Pt-Cl species for 1.08 wt% Pt/Mo<sub>2</sub>C after 120 h test. This suggests that the ca. 15 % activity loss for 1.08 wt% Pt/Mo<sub>2</sub>C after long-term operation is likely due to Pt<sup>2+</sup> reduction to atomic-like Pt<sup>δ+</sup>. In addition, the further STEM observation for Pt/Mo<sub>2</sub>C composite catalyst after long-term cycling found that the majority of Pt clusters anchored on Mo<sub>2</sub>C still maintain their initial combing state (Figure 5d). The above electrocatalytic results indicates that the prepared Pt/Mo<sub>2</sub>C catalysts indeed possess extremely high activity and excellent stability due to the highly dispersed ultrathin layer of Pt cluster active species, as well as the strong interaction between the Pt clusters and Mo<sub>2</sub>C substrate.

## Conclusions:

In summary, we have clearly demonstrated a novel composite electrocatalyst composed of atomic layers of Pt clusters strongly anchored on  $\beta$ -Mo<sub>2</sub>C nanorod (Pt/Mo<sub>2</sub>C) through both theoretically and experimentally routes, resulting into nearly 0 V onset potential. Remarkably, Pt/Mo<sub>2</sub>C with extremely low Pt loading of 1.08 wt% exhibits 10 folds better mass activity compared to the widely used reference 20 wt% Pt/C in acidic media. This catalyst also displays 25 folds and 15 folds better activity than 20 wt% Pt/C in neutral and alkaline media, respectively. Additionally, 1.08 wt% Pt/Mo<sub>2</sub>C presents a considerable durability in a wide pH range. The superior HER activity is very likely due to the well-dispersed atomic layers of Pt clusters, leading to a high Pt utilization efficiency. Furthermore, the Pt clusters strongly anchored on Mo<sub>2</sub>C brings a strong interaction between surface such clusters and Mo<sub>2</sub>C substrate and thus results in a robust catalyst against to electrochemical corrosion, leading to nearly 120 h stability, much better than commercial 20 wt% Pt/C. The rational design strategy can be extended to produce other highly active, low-cost, scalable electrocatalysts and Pt/Mo<sub>2</sub>C composite catalysts would highlight great promise for practical applications in the fields of energy conversion and storage.

## Conflicts of interest

The authors declare no conflict of interest.

## Acknowledgements

This work is supported by the National Science Funding Committee (NSFC, No. 21573204, 21421063), MOST (2016YFA0200602, 2018YFA0208600), Fundamental Research Funds for the Central Universities, National Program for Support of Top-notch Young Professional, Anhui Initiative in Quantum Information Technologies, and the fund of the State Key Laboratory of Solidification Processing in NWPU (No. SKLSP201845). We are also thankful for the funding from State Key Laboratory of Solidification Processing in NWPU (No. SKLSP201613). C. Jiang and J. Tang are thankful for Royal Society-Newton Advanced Fellowship grant (NA170422) and the Leverhulme Trust (RPG-2017-122).

## Notes and references

‡ Footnotes relating to the main text should appear here. These might include comments relevant to but not central to the matter under discussion, limited experimental and spectral data, and crystallographic data.

- S. Chu, A. Majumdar, *Nature* **2012**, 488, 294-303.
- T. R. Cook, D. K. Dogutan, S. Y. Reece, Y. Surendranath, T. S. Teets, D. G. Nocera, *Chem. Rev.* **2010**, 110, 6474-6502.
- H. J. Yan, Y. Xie, Y. Q. Jiao, A. P. Wu, C.G. Tian, X. M. Zhang, L. Wang, H.G. Fu, *Adv. Mater.* **2018**, 30, 1704156.
- H. Jin, X. Liu, Y. Jiao, A. Vasileff, Y. Zheng, S. Qiao, *Nano Energy* **2018**, 53, 690-697
- Y. C. Kimmel, X. Xu, W. Yu, X. Yang, J. G. Chen, *ACS Catal.* **2014**, 4, 1558-1562.
- B. M. Tackett, W. Sheng, J. G. Chen, *Joule* **2017**, 1, 253-263.
- D. V. Esposito, S. T. Hunt, A. L. Stottlemeyer, K. D. Dobson, B. E. McCandless, R. W. Birkmire, J. G. Chen, *Angew. Chem. Int. Ed.* **2010**, 49, 9859-9862.
- D. V. Esposito, S. T. Hunt, Y. C. Kimmel, J. G. Chen, *J. Am. Chem. Soc.* **2012**, 134, 3025-3033.
- M. Miao, J. Pan, T. He, Ya. Yan, B. Y. Xia, X. Wang, *Chem. Eur. J.* **2017**, 23, 10947-10961.
- L. Wang, E. G. Mahoney, S. Zhao, B. Yang, J. G. Chen, *Chem. Commun* **2016**, 52, 3697-3700.
- R. B. Levy, M. Boudart, *Science* **1973**, 181, 547-549.
- J. R. Kitchin, J. K. Nørskov, M. A. Barteau, J. G. Chen, *Catal. Today* **2005**, 105, 66-73.
- N. M. Schweitzer, J. A. Schaidle, O. K. Ezekoye, X. Q. Pan, S. Linic, L. T. Thompson, *J. Am. Chem. Soc.* **2011**, 133, 2378-2381.
- J. Li, L. T. Liu, Y. Liu, M. Z. Li, Y. H. Zhu, H. C. Liu, Y. Kou, J. Z. Zhang, Y. Han, D. Ma, *Energy Environ. Sci.* **2014**, 7, 393-398.
- L. Lin, W. Zhou, R. Gao, S. Yao, X. Zhang, W. Xu, S. Zheng, Z. Jiang, Q. Yu, Y. W. Li, C. Shi, X. D. Wen, D. Ma, *Nature* **2017**, 544, 80-83.
- B. M. Tackett, Y. C. Kimmel, J. G. Chen, *Int. J. Hydrog. Energy* **2016**, 41, 5948-5954.
- S. Saha, B. Martin, B. Leonard, D. Li, *J. Mater. Chem. A.* **2016**, 4, 9253-9265.
- T. G. Kelly, K. X. Lee, J. G. Chen, *J. Pow. Source.* **2014**, 271, 76-81.
- C. Wan, Y. N. Regmi, B. M. Leonard, *Angew. Chem. Int. Ed.* **2014**, 53, 6407-6410.
- J. K. Nørskov, T. Bligaard, A. Logadottir, J. R. Kitchin, J. G. Chen, S. Pandalov, U. Stimming, *J. Electrochem. Soc.* **2005**, 152, J23-J26.
- B. Hinnemann, P. G. Moses, J. Bonde, K. P. Jørgensen, J. H. Nielsen, S. Hørch, I. Chorkendorff, J. K. Nørskov, *J. Am. Chem. Soc.* **2005**, 127, 5308-5309.
- Q. Liu, Q. Fang, W. Chu, Y. Wan, X. Li, W. Xu, M. Habib, S. Tao, Y. Zhou, D. Liu, T. Xiang, A. Khalil, X. Wu, M. Chhowalla, P. M. Ajayan, L. Song, *Chem. Mater.* **2017**, 29, 4738-4744.
- R. Zhang, Z. Sun, R. Feng, Z. Lin, H. Liu, M. Li, Y. Yang, R. Shi, W. Zhang, Q. Chen, *ACS Appl. Mater. Interfaces* **2017**, 9, 38419-38427.
- H. Li, L. Wang, Y. Dai, Z. Pu, Z. Lao, Y. Chen, M. Wang, X. Zheng, J. Zhu, W. Zhang, R. Si, C. Ma, J. Zeng, *Nat. Nanotech.* **2018**, 1, 411-417.
- B. Qiao, A. Wang, X. Yang, L. F. Allard, Z. Jiang, Y. Cui, J. Liu, J. Li, T. Zhang, *Nat Chem* **2011**, 3, 634-641.
- P. D. Nellist, M. F. Chisholm, N. Dellby, O. L. Krivanek, M. F. Murfitt, Z. S. Szilagyi, A. R. Lupini, A. Borisevich, W. H. Sides Jr, S. J. Pennycook, *Science* **2004**, 305, 1741-1741.
- S. Wang, A. Y. Borisevich, S. N. Rashkeev, M. V. Glazoff, Karl. Sohlberg, S. J. Pennycook, S. T. Pantelides, *Nat Mater.* **2004**, 3, 143-146.
- H. B. Zhang, P. F. An, W. Zhou, B. Y. Guan, P. Zhang, J. C. Dong, X. W. Lou, *Sci. Adv.* **2018**, 4, eaa06657.
- K. Tang, X. F. Wang, Q. Li, C. L. Yan, *Adv. Mater.* **2018**, 30, 1704779.
- K. Li, Y. Li, Y. Wang, J. Ge, C. Liu, W. Xing, *Energy Environ. Sci.* **2018**, 11, 1232-1239.
- H. Yoshida, Y. Yazawa, N. Takagi, A. Satsuma, T. Tanaka, S. Yoshida, T. Hattori, *J. Synchrotron Radiation.* **1999**, 6, 471-473.
- J. X. Diao, W. Y. Yuan, Y. Su, Y. Qiu, X. H. Guo, *Adv. Mater. Interf.* **2018**, 1800223.
- Y. Y. Ma, C. X. Wu, X. J. Feng, H. Q. Tan, L. K. Yan, Y. Liu, Z. H. Kang, E. B. Wang, Y. G. Li, *Energy Environ. Sci.* **2017**, 10, 788-798.
- Y. Huang, Q. Gong, X. Song, Kun. Feng, K. Nie, F. Zhao, Y. Wang, M. Zeng, J. Zhong, Y. Li, *ACS Nano* **2016**, 10, 11337-11343.
- Z. Shi, K. Nie, Z. J. Shao, B. Gao, H. Lin, H. Zhang, B. Liu, Y. Wang, Y. Zhang, X. Sun, X. M. Cao, P. Hu, Q. Gao, Y. Tang, *Energy Environ. Sci.* **2017**, 10, 1262-1271.
- X. Fan, Y. Liu, Z. Peng, Z. Zhang, H. Zhou, X. Zhang, B. I. Yakobson, W. A. Goddard, X. Guo, R. H. Hauge, *ACS Nano* **2017**, 11, 384-394.
- L. F. Pan, Y. H. Li, S. Yang, P. F. Liu, M. Q. Yu, H. G. Yang, *Chem. Commun.* **2014**, 50, 13135-13137.
- H. Lin, Z. Shi, S. He, X. Yu, S. Wang, Q. Gao, Y. Tang, *Chem. Sci.* **2016**, 7, 3399-3405.
- M. Fan, H. Chen, Y. Wu, L. L. Feng, Y. Liu, G. D. Li, X. Zou, *J. Mater. Chem. A.* **2015**, 3, 16320-16326.
- J. S. Li, Y. Wang, C. H. Liu, *Nat. Commun.* **2016**, 7, 11204.
- H. Zhang, Z. Ma, G. Liu, L. Shi, J. Tang, H. Pang, K. Wu, T. Takei, J. Zhang, Y. Yamauchi, J. Ye, *NPG Asia Mater.* **2016**, 8, e293.
- J. Deng, H. Li, S. Wang, D. Ding, M. Chen, C. Liu, Z. Tian, K. S. Novoselov, Chao. Ma, D. Deng, X. Bao, *Nat. Commun.* **2017**, 8,14430.
- H. B. Wu, B. Y. Xia, L. Yu, X. Y. Yu, X. W. Lou, *Nat. Commun.* **2015**, 6, 6512.

